

## **DI AND TRIVALENT IONS CO-SUBSTITUTED HYDROXYAPATITE NANOPARTICLES: SYNTHESIS, CHARACTERIZATION, ANTIBACTERIAL ACTIVITY AND IN VITRO STUDIES**

**Sivalingam Lakshmanan**

Department of Chemistry, BIHER, Bharath University, Chennai 600 073, India

E-mail:lachuchem666@gmail.com

### **Abstract**

The present work is aimed at the synthesis of antibacterial and bioactive both divalent and trivalent substituted hydroxyapatite ( $\text{LaM}\text{Ca}_3(\text{PO}_4)_3\text{OH}$ ,  $\text{La}_{0.7}\text{M}_{0.3}\text{Ca}_4(\text{PO}_4)_3\text{OH}$  ( $\text{M} = \text{Sr}, \text{Zn}, \text{Mg}$ )) were synthesized by ultra sonic method. The as-synthesized samples were characterized by Fourier transform infrared spectroscopy (FTIR), X-ray diffraction (XRD), field emission scanning electron microscopy (FESEM), energy dispersive X-ray analysis (EDAX), high resolution transmission electron microscopy (HRTEM) and thermo gravimetric analysis (TGA). The antibacterial activity of the as-synthesized nanoparticles was evaluated against two prokaryotic strains (*Escherichia coli* and *Staphylococcus aureus*).

### **Introduction**

The most significant role of biometrics is to make possible a function of the human body in a safe, reliable and physiologically suitable manner without causing any adverse effects [1]. Hydroxyapatite [ $\text{Ca}_{10}(\text{PO}_4)_6(\text{OH})_2$ , HA], the major constituent of bone and teeth has involved a great deal of attention in biomedical applications owing to its close likeness in chemical composition with the mineral part of natural bone and teeth [1]. HA has outstanding properties including biocompatibility, bioactivity, osteointegrity, osseous inductivity, osteoconductivity [3] and ability to form a direct chemical bond with human hard tissues [5,6]. Unfortunately, pure HA possesses several limitations which also include lack of antibacterial activity that undermines its long term stability and causes implant failures. This causes the increased risk of bacterial adherence and colonization of the implants coated with HAP. Hence, the addition of the inorganic antibacterial agents into pure HAP is adopted to ensure the success of the implants coated with HAP. In addition, due to the above-mentioned prominent properties, various types of HAP-based antibacterial property composites, coatings and thin films have been extensively developed and used for biomedical applications by many researchers [8–13].

Lanthanide (La) can act similar to calcium in organisms, so it accumulates in bones in small amounts, therefore, La-containing compounds can stimulate metabolism in organisms [26,27]. The electronegativity of metallic La is 1.06, while the ionic radius of  $\text{La}^{3+}$  is 0.107 nm. Both values are close to those of Ca (1.01 and 0.100 nm for  $\text{Ca}^{2+}$ , respectively). Therefore,  $\text{La}^{3+}$  may replace  $\text{Ca}^{2+}$  in the lattice of HAp. In addition, trivalent  $\text{Bi}^{3+}$  cations possess some antibacterial properties, which are beneficial for biomedical applications [28]. In recent years the incorporation of inorganic antibacterial agents like silver ( $\text{Ag}^+$ ), copper ( $\text{Cu}^{2+}$ ), zinc ( $\text{Zn}^{2+}$ ), titanium ( $\text{Ti}^{4+}$ ) cerium ( $\text{Ce}^{3+}$ ) and bismuth ( $\text{La}^{3+}$ ) in biomaterials for the prevention of microbial infection is followed [12–14]. Among these ions,  $\text{La}^{3+}$  is believed to have superior chemical and physical properties such as biocompatibility, high thermal stability, high mechanical stability and also antiseptic, astringent, protective, antacid, antisecretory, local gastrointestinal properties, non-toxic to human cells at low concentration [15,16].  $\text{La}^{3+}$  exhibit high antibacterial activity by maintaining low cytotoxicity [17]. It has been demonstrated that the higher level of  $\text{La}^{3+}$  in the material gives better antimicrobial effect, but with increasing cytotoxicity [18]. It is therefore necessary to incorporate a secondary material to lessen the negative effects by maintaining the antimicrobial properties of  $\text{La}^{3+}$ . There are minerals like strontium (Sr), magnesium (Mg), zinc (Zn) and traces of metal elements that accelerate bone formation [19,20].

**Synthesis of HA, M-HA and M/La-HA**

HAP, different concentrations of M-HAP and M/La-HAP were synthesized by microwave irradiation method using a  $\text{Ca}(\text{NO}_3)_2 \cdot 4\text{H}_2\text{O}$ ,  $(\text{NH}_4)_2\text{HPO}_4$ ,  $(\text{La}(\text{NO}_3)_3 \cdot 5\text{H}_2\text{O})$  and  $\text{Mg}(\text{NO}_3)_2 \cdot 6\text{H}_2\text{O}$ , respectively. Three series of particles were synthesized with same phosphorus sources, for series 1 (HAP): using  $\text{Ca}(\text{NO}_3)_2 \cdot 4\text{H}_2\text{O}$  and  $(\text{NH}_4)_2\text{HPO}_4$ , series 2 (M-HAP): using  $\text{Ca}(\text{NO}_3)_2 \cdot 4\text{H}_2\text{O}$ ,  $\text{Sr}(\text{NO}_3)_2 \cdot 6\text{H}_2\text{O}$ ,  $\text{Zn}(\text{NO}_3)_2 \cdot 6\text{H}_2\text{O}$ ,  $\text{Mg}(\text{NO}_3)_2 \cdot 6\text{H}_2\text{O}$  and  $(\text{NH}_4)_2\text{HPO}_4$  and series 3 (M/La-HAP): using  $\text{Ca}(\text{NO}_3)_2 \cdot 4\text{H}_2\text{O}$ ,  $(\text{La}(\text{NO}_3)_3 \cdot 5\text{H}_2\text{O})$ ,  $\text{Sr}(\text{NO}_3)_2 \cdot 6\text{H}_2\text{O}$ ,  $\text{Zn}(\text{NO}_3)_2 \cdot 6\text{H}_2\text{O}$ ,  $\text{Mg}(\text{NO}_3)_2 \cdot 6\text{H}_2\text{O}$  and  $(\text{NH}_4)_2\text{HPO}_4$ .

HA nanoparticle is prepared by dissolving  $\text{Ca}(\text{NO}_3)_2 \cdot 4\text{H}_2\text{O}$  in double distilled water to 0.5 M (solution 1) and the pH was adjusted to 9 using NaOH solution and  $(\text{NH}_4)_2\text{HPO}_4$  was dissolved in double distilled water to 0.3 M (solution 2). Solution 2 was added drop by drop to solution 1 and stirred for 2 h and the pH was constantly adjusted and maintained at 9 using NaOH solution during the reaction. After mixing, the obtained

precipitate was kept in a microwave oven (2.45 GHz, LG, India) at 720 W and irradiated with microwave for 10 min. To obtain the white precipitate,  $\text{NH}_4^+$  and  $\text{NO}_3^-$  ions were removed by washing the precipitate repeatedly with deionised water, filtered and then dried at 120 °C for about 12 h in hot air oven. Finally, the dried white powder was calcined and sintered in a muffle furnace at 800 °C for 3 h.

**Sample characterization**

The functional groups present in the as-synthesized samples were analyzed by Nicolet 380 FT-IR Spectrometer (Perkin Elmer, USA) over the range from  $4000\text{ cm}^{-1}$  to  $400\text{ cm}^{-1}$  with a number of scans 32 and resolution  $4\text{ cm}^{-1}$ . The test samples were prepared by mixing 0.01 g of as-synthesized powders together with 1 g of KBr to make a pellet.

X-ray Diffraction (XRD, Seifert, X-ray diffractometer Siemens D500 Spectrometer, with Cu K $\alpha$  radiation generated at 35 kV and 25 mA) was employed to identify the crystalline phase composition of the as-synthesized materials. The morphologies and elemental analysis of the as prepared powders (HAP, M-HA and M/La-HA) were determined using a SEM equipped with EDAX (JEOL JSM-5610).

**Antibacterial activity**

The in vitro antibacterial activity of the as-synthesized pure HA, M-HA and M/La-HA (with different  $\text{La}^{3+}$  concentrations of 0.05, 0.075 and 0.1 M) nanoparticles has been investigated against E.coli and S. aureus as the model Gram-negative bacteria and Gram-positive bacteria by the agar disc diffusion method [19]. The inoculums of the two microorganisms such as E.coli and S. aureus were prepared from fresh overnight broth cultures (Tryptone soy broth with 0.6% yeast extract– Torlak, Serbia) that were incubated at 37 °C with constant stirring and they were used for the diffusion studies. The agar disc diffusion test was performed at Muller-Hinton agar and it was carried out by pouring agar into petri dishes to form 4 mm thick layers. Further, by adding 2 ml thick inoculums of the test organisms of E. coli and S. aureus in order to obtain semi confluent growth. Petri dishes were left for 10 min to dry in air and after that, discs (6 mm) were prepared from Whatman filter paper and immersed into different volumes of (25, 50, 75, 100, 125  $\mu\text{l}$ ) as synthesized HA, M-HA and M/La-HA (with different  $\text{La}^{3+}$  concentrations of 0.05, 0.075 and 0.1 M) nanoparticles. Then the discs were placed at equal distance and incubated for 24 h at 37 °C. After incubation, antibacterial activity was measured as zone of inhibition (mm) around the disc which was produced by the as-synthesized samples against the two prokaryotic strains.

**Apatite forming ability of M/La-HA in SBF**

The apatite forming ability of the as-synthesized M/La-HA at optimum concentration of  $\text{La}^{3+}$  (0.1 M) were studied by immersion the compacted pellets (samples) in Simulated Body Fluid (SBF) at 37 °C for various days. The SBF was described by Kokubo et al., [20]. The ionic concentration of human blood plasma and that of the

SBF is given in Table. 1. The appropriate amount of analytical grade reagents were mixed together and 1 M HCl was used to maintain pH of the solution at 7.4 to mimic the concentration of human blood plasma. Then, the pellets were soaked in 40 ml of SBF in beaker with airtight lids for various days like 7, 14 and 21 days at  $37 \pm 0.5$  °C in an incubator. The SBF solution was renewed every three days for a period of 7, 14 and 21 days to avoid any change in cationic concentration that may occur due to degradation of the sample. The immersed pellets were then gently washed with de-ionized water and the formation of bone-like apatite on the samples was evaluated by FESEM.

### **3.1 Structural characterizations of the as-synthesized samples**

#### **3.1.1 FTIR analysis**

Representative FTIR spectra of the as-synthesized HA, M-HA and M/La-HA (with different  $\text{La}^{3+}$  concentrations of 0.05, 0.075 and 0.1 M) nanoparticles are shown in Fig. 1(a)-(e). The characteristic peaks (Fig. 1(b)) appeared at 1016 and 1080  $\text{cm}^{-1}$ , 592  $\text{cm}^{-1}$  and 559  $\text{cm}^{-1}$ , 472  $\text{cm}^{-1}$  as well as the band observed at 947  $\text{cm}^{-1}$  are assigned to the phosphate groups [21, 22]. The absorption peaks observed at 3590 and 639  $\text{cm}^{-1}$  are assigned to the stretching and bending vibration of the hydroxyl ( $\text{OH}^-$ ) groups. Furthermore, the broad stretching band at 3440  $\text{cm}^{-1}$  and a bending peak at 1620  $\text{cm}^{-1}$  are attributed to the water molecule of M-HA sample, respectively. FTIR spectrum of M-HA nanoparticles (Fig. 1(b)) shows a similar structure as that of pure HA [23, 24], but with a change in the IR wave numbers of bands. The spectra obtained for the M/La-HA (with different  $\text{La}^{3+}$  concentrations of 0.05, 0.075 and 0.1 M) powders show a similar structure (Fig. 1(c)-(e)) like M-HA nanoparticles. For the M/La-HA sample (with optimum (0.1 M) concentration of  $\text{La}^{3+}$ ), the FTIR spectrum as shown in Fig. 1(e) depicts the formation of M/La-HA. For instance, the characteristic fundamental vibrational modes of the phosphate peaks appeared at 1016 and 1079  $\text{cm}^{-1}$ , 591  $\text{cm}^{-1}$  and 558  $\text{cm}^{-1}$ , 471  $\text{cm}^{-1}$  as well as the bands are observed at 946  $\text{cm}^{-1}$ . Apart from these, the broad stretching band at 3441  $\text{cm}^{-1}$  and a bending band at 1621  $\text{cm}^{-1}$  are attributed to the stretching and bending mode of water molecule, while the absorption bands at 3589  $\text{cm}^{-1}$  and 638  $\text{cm}^{-1}$  are assigned to the stretching and bending vibration of  $\text{OH}^-$  groups of M/La-HA, respectively.

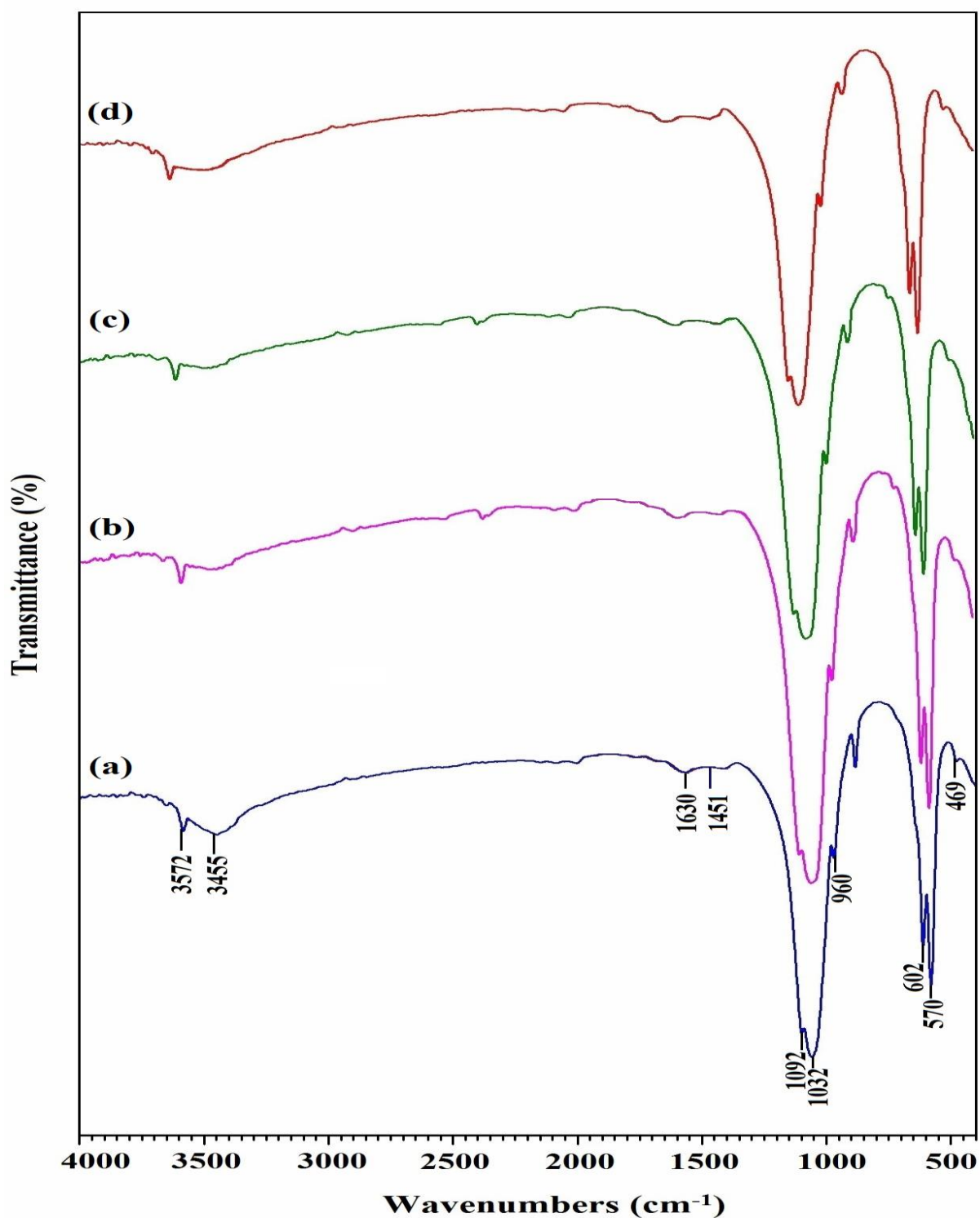


Fig.1. FT-IR spectra of (a) HAP ,M- HAP powders and different La<sup>3+</sup> concentrations of M- HAP (b) 0.5 wt% (c) 1.5 wt% (d) 2.5 wt%.

### 3.1.2 XRD analysis

The XRD patterns of the as-synthesized nanoparticles HA, M-HA and M/La-HA (with different La<sup>3+</sup> concentrations of 0.05, 0.075 and 0.1 M) nanoparticles are shown in Fig. 2(a)-(e).The major diffraction peaks

identified for M/La-HA and M-HA are in good agreement with the standard data for HA (ICDD card No. 09-0432). Fig. 2(c)-(e) depicts the XRD patterns obtained for the M/La-HA (with different La<sup>3+</sup> concentrations of 0.05, 0.075 and 0.1 M) nanoparticles. Wide and intense peaks (Fig. 2(e)) are observed at 2θ values of 25.9°, 31.9°, 32.5° and 32.9° for M/La-HA nanoparticles and no other secondary peaks are found. As the Bi<sup>3+</sup> concentration is increased (Fig. 2(c)-(e)), the diffraction peaks become wide indicating the decreased crystallinity as well as particle size due to the of La<sup>3+</sup> in M-HA sample [14,15, 25]. However, the broad peaks display that the obtained M/La-HA particles were not well crystallized or) in nanosize. Whereas for the M-HA (Fig. 2(b)), the diffraction peak positions deviated slightly from the standard XRD patterns for HA, indicating the substitution of Mg, Sr and Zn [9] into the pure HA sample. The above results are further substantiated by the calculation of particle size using Debye-Scherrer's equation and the obtained values are presented in Table.2.

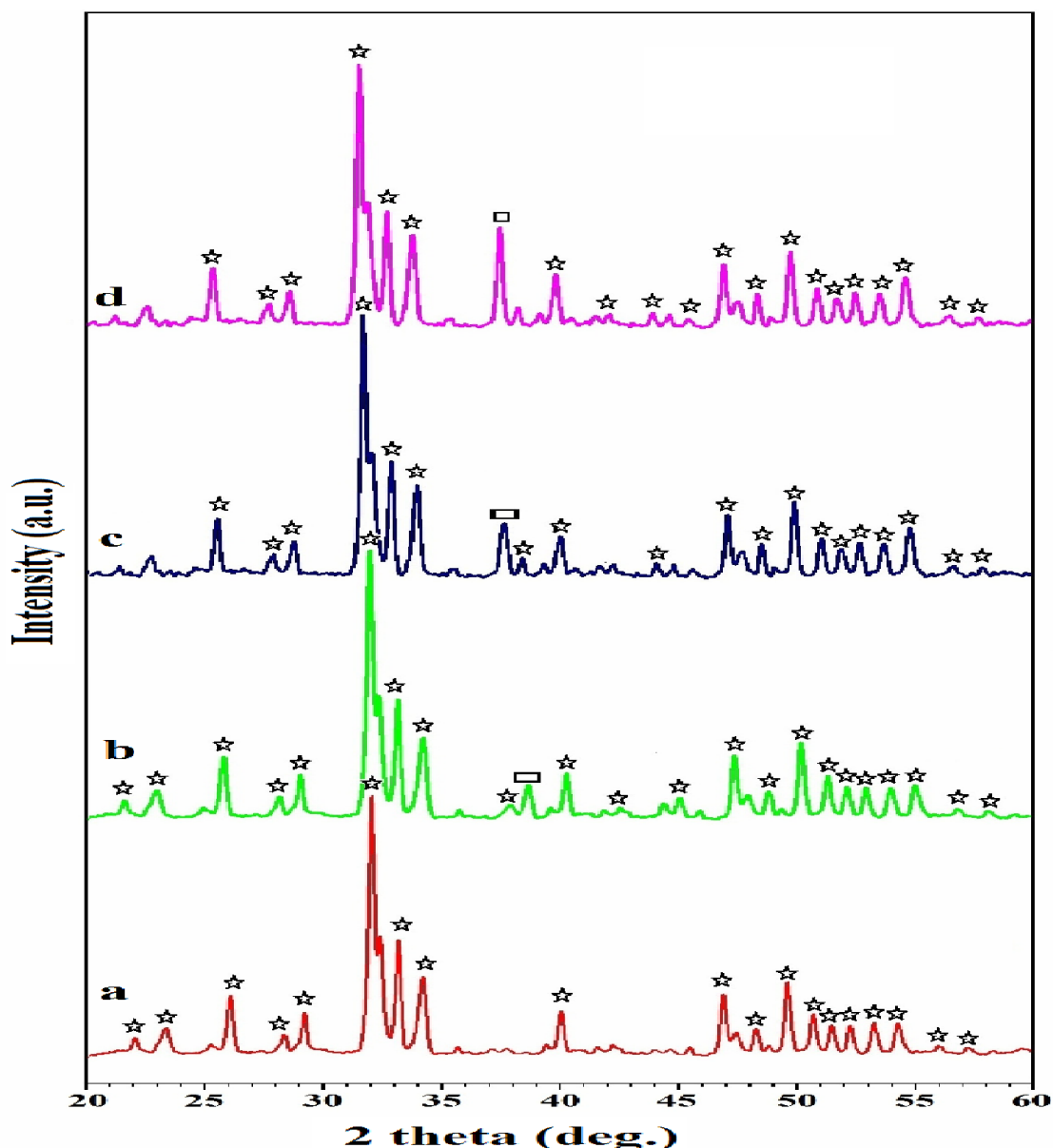


Fig. 2. XRD patterns of (a) HAP and different concentrations of La substituted M-HAP powders (b) 0.5 wt% (c) 1.5 wt% (d) 2.5 wt%.

## Conclusion

In summary, novel bioactive and antibacterial Mg/Bi-HA nanoparticles were synthesized successfully by ultrasonic irradiation method. The structural characterization clearly revealed the formation of HA, M-HA and M/La-HA (with different La<sup>3+</sup> concentrations of 0.05, 0.075 and 0.1 M) nanoparticles. The crystallinity and size of the pure HA nanoparticles are decreased on the substitution of the Mg<sup>2+</sup>, Sr<sup>2+</sup>, Zn<sup>2+</sup> and La<sup>3+</sup> and are evident from the XRD and HRTEM results. The substitution of M-HA by different concentrations (0.05, 0.075 and 0.1M) of La<sup>3+</sup> significantly improved the antibacterial activity of M/La-HA nanoparticles. The antibacterial results reveal that the as-synthesized M/La-HA (with 0.1 M La<sup>3+</sup>) powder exhibited a strong antibacterial activity against the E. Cole and S. Areas. Moreover, the presence of minerals and La<sup>3+</sup> in M/La-HA nanoparticles improved the thermal stability up to 1200 °C. In vitro apatite forming ability test evidenced the regulating effect of minerals and Bi<sup>3+</sup> on the apatite formation. As a result, these M/La-HA nanoparticles synthesized by ultrasonic irradiation method can serve as a very promising biomaterial for biomedical applications.

## References

1. M. Vallet-Regi, D. Arcos, Biomimetic nanoceramics in clinical use: From materials to applications, RSC Publishing, UK, 2008.
2. M. Vallet Regí, Where do we come from and which are the future expectations, Key Eng. Mater. 377 (2008) 1-18.
3. G. Tripathi, P. Choudhury, B. Basu, Development of polymer based biocomposites: a review, Mater. Technol. 25 (2010) 158-176.
4. R.Z. LeGeros, Calcium phosphate-based osteoinductive materials, Chem. Rev. 108 (2008) 4742-4753.
5. I. Smiciklas, A. Onjia, J. Markovi, S. Raicevi, Comparison of hydroxyapatite sorption properties towards cadmium, lead, zinc and strontium ions, Mater. Sci. Forum 494 (2005) 405-410.
6. E.D. Berry, G.R. Siragusa, Hydroxyapatite adherence as a means to concentrate bacteria, Appl. Environ. Microbiol. 63 (1997) 4069-4074.
7. M. Vallet-Regi, J.M. Gonzalez-Calbet, Calcium phosphates as substitution of bone tissues, Prog. Solid State Chem. 32 (2004) 1-31.
8. S. Atmaca, K. Gul, R. Clcek, The effect of zinc on microbial growth, Turk. J. Med. Sci. 28 (1998) 595-597.
9. B. Sugarman, Zinc and infection, Rev. Infect. Dis. 5 (1983) 137-147.
10. T.N. Phan, T. Bucker, J. Sheng, J.D. Baldeck, R.E. Marquis, Physiologic actions of zinc related to inhibition of acid and alkali production by oral streptococci in suspensions and biofilms and enhanced peroxide killing, Oral Microbiol. Immun. 19 (2004) 31-38.
11. W. Chen, Y. Liu, H.S. Courtney, M. Bettenga, C.M. Agrawal, J.D. Bumgardner, J.L. Ong, In vitro antibacterial and biological properties of magnetron co-sputtered silver-containing hydroxyapatite coating, Biomaterials 27 (2006) 5512-5517.
12. F. Heidenau, W. Mittelmeier, R. Detsch, M. Haenle, F. Stenzel, G. Ziegler, H. Gollwitzer, A novel antibacterial titania coating: Metal ion toxicity and in vitro surface colonization, J. Mater. Sci. Mater. Med. 16 (2005) 883-888.

13. R.J. Chung, M.F. Hsieh, C.W. Huang, L.H. Perng, H.W. Wen, T.S. Chin, Anti-microbial hydroxyapatite particles synthesized by a sol-gel route, *J. Biomed. Mater. Res. B* 76 (2006) 169-178.
14. A. Ewald, D. Hosel, S. Patel, L.M. Grover, J.E. Barralet, U. Gbureck, Silver-doped calcium phosphate cements with antimicrobial activity, *Acta Biomater.* 7 (2011) 4064-4070.
15. K. Jamuna-Thevi, S. Bakar, S. Ibrahim, N. Shahab, M. Toff, Quantification of silver ion release, in vitro cytotoxicity and antibacterial properties of nanostructured Ag doped TiO<sub>2</sub> coatings on stainless steel deposited by RF magnetron sputtering, *Vacuum* 86 (2011) 235-241.
16. D. Gopi, S. Nithiya, E. Shinyjoy, L. Kavitha, Spectroscopic investigation on formation and growth of mineralized nanohydroxyapatite for bone tissue engineering applications, *Spectrochim. Acta A: Mol. Biomol. Spectrosc.* 92 (2012) 194-200.
17. J. Buehler, P. Chappuis, J.L. Saffar, Y. Tsouderos, A. Vignery, Strontium ranelate inhibits bone resorption while maintaining bone formation in alveolar bone in monkeys (*Macaca fascicularis*), *Bone* 29 (2001) 76-79.
18. S. Peng, G. Zhou, Z. Li, K.M.C. Cheung, K.D.K. Luk, Z. Zhou, W.W. Lu, Strontium promotes osteogenic differentiation of mesenchymal stem cells through enhancing the Raserk Mapk Signalling, *Cell. Physiol. Biochem.* 23 (2009) 165-174.
19. E. Landi, A. Tampieri, M. Mattioli-Belmonte, G. Celotti, M. Sandri, A. Gigante, P. Fava, G. Biagini, Biomimetic Mg- and Mg<sub>2</sub>CO<sub>3</sub>- substituted hydroxyapatites: Synthesis characterization and in vitro behaviour, *J. Eur. Ceram. Soc.* 26 (2006) 2593-2601.
20. M. Percival, Bone health and osteoporosis, *Appl. Nutr. Sci. Rep.* 5 (1999) 1-5.
21. A. Bigi, G. Falini, E. Foresti, A. Ripamonti, M. Gazzano, N. Roveri, Magnesium influence on hydroxyapatite crystallization, *J. Inorg. Biochem.* 49 (1993) 69-78.
22. E. Bertoni, A. Bigi, G. Cojazzi, M. Gandolfi, S. Panzavolta, N. Roveri, Nanocrystals of magnesium and fluoride substituted hydroxyapatite, *J. Inorg. Biochem.* 72 (1998) 29-35.
23. S.R. Kim, J.H. Lee, Y.T. Kim, D.H. Riu, S.J. Jung, Y.J. Lee, S.C. Chung, Y.H. Kim, Synthesis of Si, Mg substituted hydroxyapatites and their sintering behaviors, *Biomaterials* 24 (2003) 1389-1398.
24. W.L. Suchanek, K. Byrappa, P. Shuk, R.E. Riman, V.F. Janas, K.S. TenHuisen, Preparation of magnesium-substituted hydroxyapatite powders by the mechanochemical- hydrothermal method, *Biomaterials* 25 (2004) 4647-4657.
25. E. Landi, G. Logroscino, L. Proietti, A. Tampieri, M. Sandri, S. Sprio, Biomimetic
26. Mg-substituted hydroxyapatite: from synthesis to in vivo behavior, *J. Mater. Sci. Mater. Med.* 19 (2008) 239-247.

### Research Highlights

✓ Synthesis of anti bacterial and bioactive M/La-HA nanoparticles by ultrasonic irradiation method is achieved

Minerals equalizes the toxic nature of La and provides better bioactivity.